https://doi.org/10.3311/PPee.22832

Periodica Polytechnica Electrical Engineering and Computer Science, 68(3), pp. 283–294, 2024

Control and Performance Analysis of an Indirect Matrix Converter Fed Triple Star Induction Motor

Ahmed Azib[1*], Adel Oubelaid[1], Djamel Ziane[1,2], Mohamed Fouad Benkhoris[2]

[1] Laboratoire de Technologie Industrielle et de l'information (LTII), Faculté de Technologie, Université de Bejaia, 06000 Bejaia, Algeria
[2] Nantes Université, Institut de Recherche en Énergie Électrique de Nantes, Atlantique, IREENA, UR 4642, 44600 Saint-Nazaire, France
[*] Corresponding author, e-mail: ahmed.azib@univ-bejaia.dz

Received: 19 June 2023, Accepted: 25 March 2024, Published online: 27 May 2024

Abstract

Efficient operation is a recommended factor in most of industrial applications. In this paper, an indirect matrix converter (IMC) topology is developed and proposed to substitute the classical (AC/DC/AC) three phase converter topologies; where the control strategy is frequently performed with a voltage source inverter (VSI). Large electrolytic capacitors are viewed as hazardous due to their short lifetime compared to ordinary capacitors and power switches, as well as their contribution to the total bulk and weight of the converter. Matrix converters may be the answer to getting rid of the capacitor, shrinking the converter, and improving its efficiency (MC). These advantages are offset by the fact that the (MC) calls for a tricky switching technique based on pulse width modulation, which is prone to commutation failure. The direct frequency conversion using the indirect matrix converter (IMC) with many advantages has appeared as an alternative to these conventional voltage inverters. This study investigates a field-oriented control (FOC) scheme for indirect matrix converter fed triple star induction motor (TSIM). After building the proposed IMC converter topology, an adequate field-oriented control strategy-based space vector modulation (SVM) is proposed and adapted for the control of the triple star induction motor. The FOC technique guarantees flux and torque decoupling while ensuring good operation performance as required in many industrial applications. The obtained numerical simulation results show and confirm the effectiveness of this control scheme.

Keywords

indirect matrix converter, voltage source inverter, matrix converters, field-oriented control, triple star induction motor, space vector modulation

1 Introduction

Electric machines play a critical role in modern industry and are an essential part of many production processes. They are used in a wide range of applications, from powering industrial machinery to providing energy for lighting and heating systems. Their high efficiency and versatility make them ideal for use in many different industries, including manufacturing, mining, and construction. The use of electric machines has greatly increased productivity and reduced the cost of production, making them an essential component of modern industry. The increasing demand for renewable energy sources has also made electric machines even more important, as they are often used in the production of clean energy. The continued development and improvement of electric machines will continue to play a major role in shaping the future of industry, making them an indispensable component of the modern manufacturing landscape.

The variable-speed drives are ubiquitous in manufacturing. AC motors are commonly used in industries. However, multiphase induction machines are increasingly employed as an alternative to conventional three-phase drives in industrial applications such as the automotive, aerospace, military, and nuclear sectors, where excellent reliability is essential. Among the many benefits of these machines are power segmentation, lower current stress on semiconductor devices, lower torque ripple, lower rotor harmonic currents and the ability to ensure safe operation. The ability to operate in a degraded mode with an acceptable torque ripple is another way a multiphase structure can boost dependability [1, 2].

Cite this article as: Azib, A., Oubelaid, A., Ziane, D., Benkhoris, M. F. "Control and Performance Analysis of an Indirect Matrix Converter Fed Triple Star Induction Motor", Periodica Polytechnica Electrical Engineering and Computer Science, 68(3), pp. 283–294, 2024. https://doi.org/10.3311/PPee.22832

This study looks at the triple star induction machine, or TSIM for short, a multiphase machine with a squirrel cage-style rotor and three sets of three-phase windings that are spatially moved by 20 electrical degrees in the stator [3–5]. Yet, induction motors are difficult to manage due to their nonlinear architectures and the link between the flux and the generated electromagnetic torque. Many methods for distinguishing the two have therefore been proposed. These algorithms are based on many hypotheses and investigations. The first vector control strategy for induction motors was called field-oriented control (FOC) [6]. FOC can be divided into two main groups: indirect and direct. To do this, the motor equations are rewritten in a coordinate system that revolves around the flux vector of the rotor. You can be guaranteed that the flux and torque will be separated using the FOC method.

During regenerative braking, energy from the machine is filtered and stored in a vast electrolytic capacitor connected to the DC link of an AC/DC/AC converter; this control approach is often implemented with a voltage source inverter (VSI). Large electrolytic capacitors are regarded as harmful because of their short lifetime compared to regular capacitors and power switches and their contribution to the converter's overall bulk and weight [7–10]. Matrix converters may be the answer to getting rid of the capacitor, shrinking the converter, and improving its efficiency (MC).

These are direct AC/AC power converters that can simultaneously change the amplitude and frequency of three-phase voltages. They have many advantages, including a smaller footprint and lower weight due to the absence of DC-link electrochemical capacitors, reversible power flow with an adjustable input power factor, and a nearly sinusoidal current flow at the input and output. These advantages are offset by the fact that the (MC) calls for a tricky switching technique based on pulse width modulation, which is prone to commutation failure [11–13].

Instead of using a traditional matrix converter, which has the drawbacks listed above, an indirect matrix converter topology (IMC) can be employed, which has all the benefits of a traditional matrix converter (MC). However, the primary use of IMC over a traditional matrix converter is the simplified commutation process. All load side switches commutate like a standard DC/AC converter [14–18], but all line side switches operate at zero current.

This paper introduces the implementation of the indirect field oriented control for (IMC) fed (TSIM). The novelty of the proposed work is given below.

- The nonlinear behavior of the indirect matrix converter, as well as the triple star induction motor model, is critical for executing and improving the control performance of the given system. To obtain an accurate system model, a mathematical model is being developed.
- By simulation tests, the strength of the indirect field oriented technique is investigated in order to counteract the detaining effect caused by the link between the flux and the generated electromagnetic torque, reversible power flow with an adjustable input power factor, and a nearly sinusoidal current flow at the input and output.

This document is organized as follows: After the Introduction section, a description of IMC topology used to feed TSIM and its modelation are given in Section 2. The control startegy, which is indirect field oriented control is discussed in Section 3. In Section 4, the simulation results representing the analysis performances of IMCs-TSIM combination are discussed. Section 5 concludes the article.

2 Topology and Modulation for the indirect matrix converter

2.1 Topology of the IMC

Three voltage source inverters are typically used to feed a TSIM via a standard current source rectifier with dc link part. In this paper, an indirect matrix converter for TSIM is investigated, with a bidirectional current source converter on the mains side and three phase voltage inverters connected to a common imaginary dc-link, as shown in Figs. 1 and 2.

2.2 Modulation method

The indirect matrix converter's principal circuit is composed of an LC filter, bidirectional current source rectifier and three six-switch inverters. To show the quality of the waves obtained with this structure and the smooth nature of the switching, the presentation of SVM algorithm is more than necessary. This control strategy's goal is to synthesize output voltages from input voltages and input currents from output currents. The modulation is carried out by uniformly combining the switching states of the rectifier stage and the inverter stage by choosing the right vectors and establishing their duty cycles [17, 18].

This relationship describes the rectifier output voltage as a function of the input voltages. The parameters of all equations are included in (Appendix Table A.2):

$$\begin{bmatrix} v_p \\ v_n \end{bmatrix} = \begin{bmatrix} m_{ap} & m_{bp} & m_{cp} \\ m_{an} & m_{bn} & m_{cn} \end{bmatrix} \begin{bmatrix} v_a \\ v_b \\ v_c \end{bmatrix} \tag{1}$$

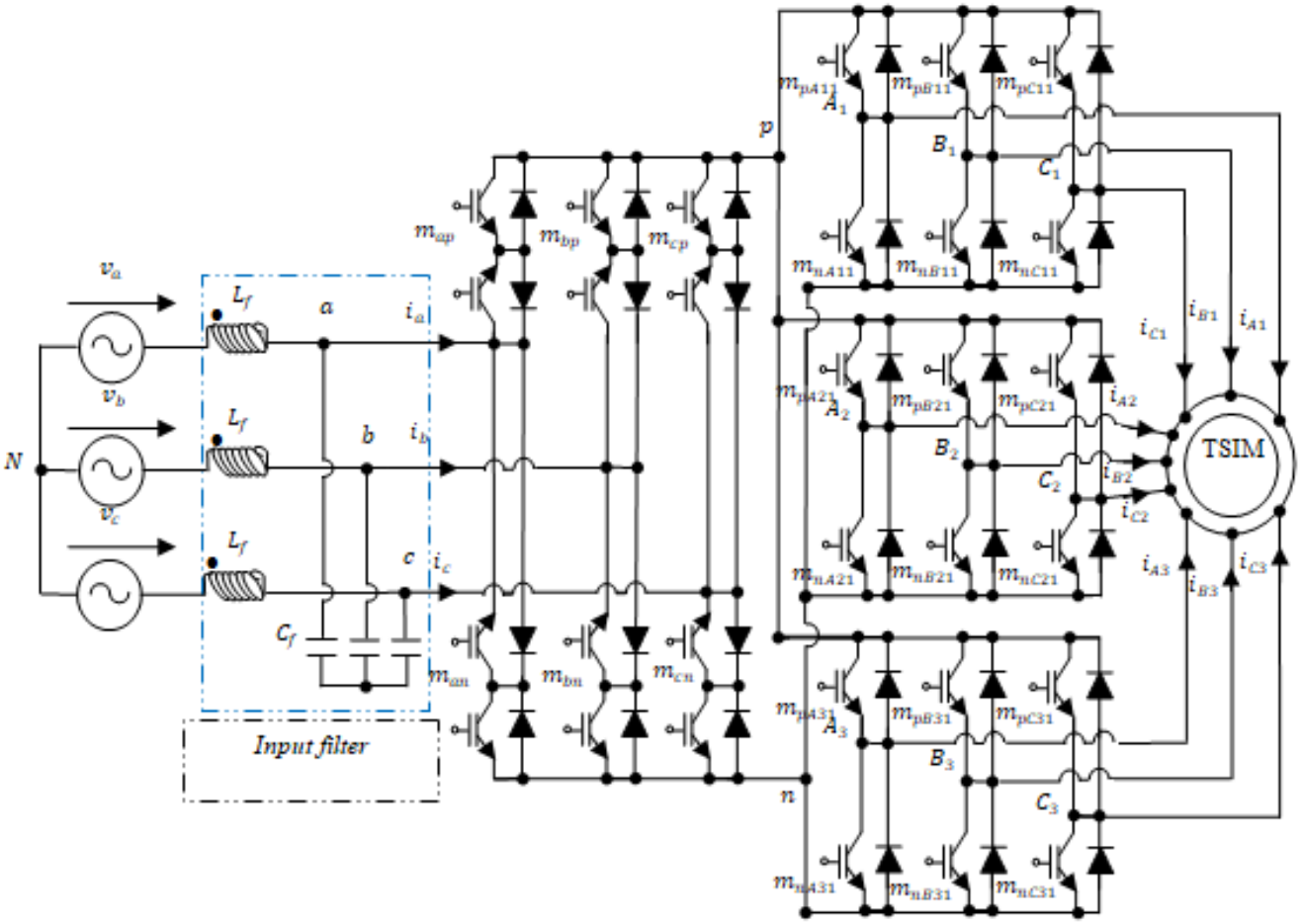

Fig. 1 Main circuit of indirect matrix converter fed TSIM

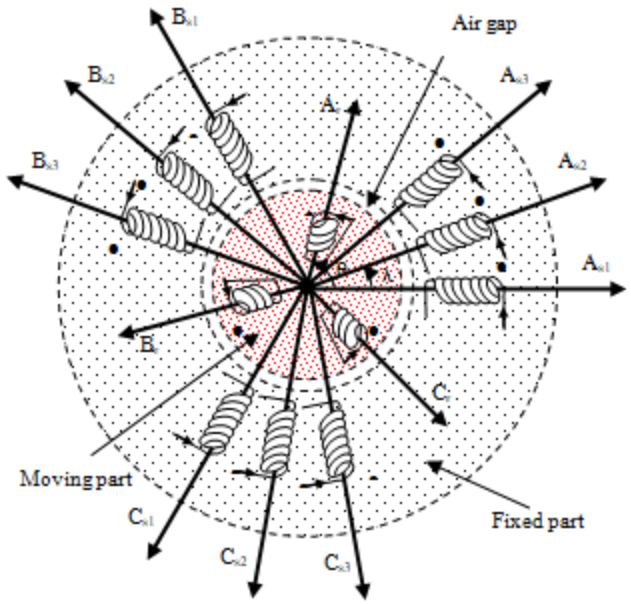

Fig. 2 Representation of the windings of TSIM

The voltage relationship for the inverters stages is provided by:

$$\begin{bmatrix} v_{Ak} \\ v_{Bk} \\ v_{Ck} \end{bmatrix} = \begin{bmatrix} m_{pAk} & m_{nAk} \\ m_{pBk} & m_{nBk} \\ m_{pCk} & m_{nCk} \end{bmatrix} \begin{bmatrix} v_p \\ v_n \end{bmatrix} \tag{2}$$

Where: $k = 1, 2, 3$

As a result, the relationship between IMC's output and input voltages is given by

$$\begin{bmatrix} v_{Ak} \\ v_{Bk} \\ v_{Ck} \end{bmatrix} = \begin{bmatrix} m_{pAk} & m_{nAk} \\ m_{pBk} & m_{nBk} \\ m_{pCk} & m_{nCk} \end{bmatrix} \begin{bmatrix} m_{ap} & m_{bp} & m_{cp} \\ m_{an} & m_{bn} & m_{cn} \end{bmatrix} \begin{bmatrix} v_a \\ v_b \\ v_c \end{bmatrix} \tag{3}$$

Where: $k = 1, 2, 3$

2.2.1 Rectifier stage control

The rectifier's bidirectional switches are regulated to prevent input line shorts, deliver DC voltage to the inverter

stage, and maintain sinusoidal input currents with the potential to control power factor. To ensure all this, the rectifier switches can only be configured in six different ways, which are then presented by six active inputs current I_1 to I_6 vectors (Fig. 3) [19, 20].

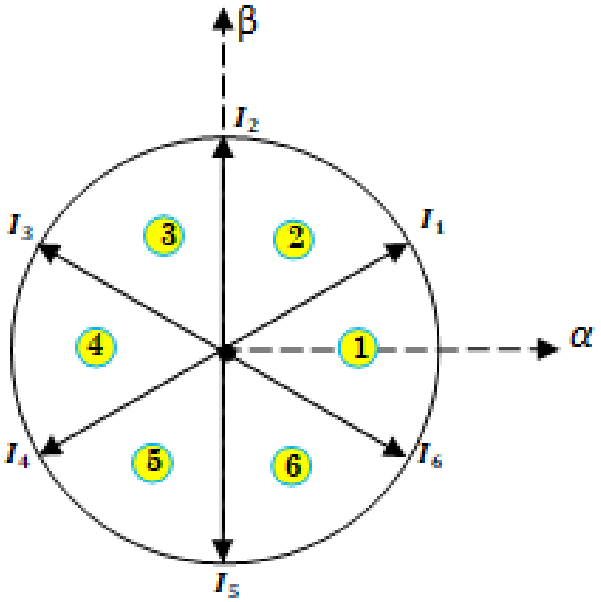

(a)

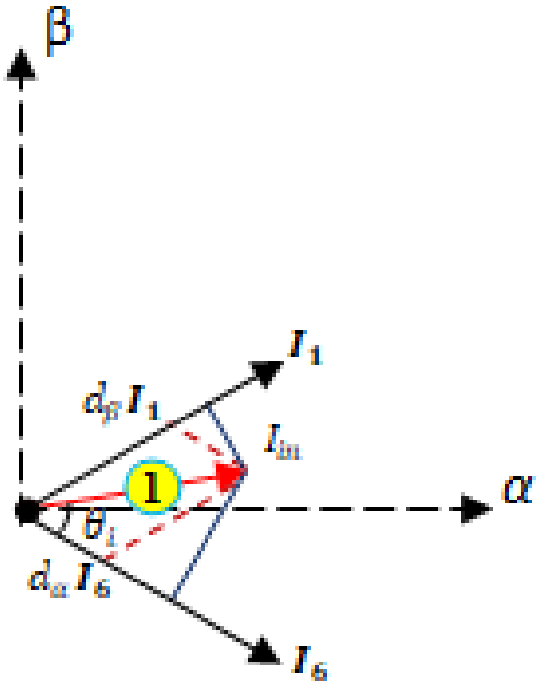

(b)

Fig. 3 Switching state vector of current source rectifier (a) and its SVM in sector **1** (b)

During a switching phase, I_{in} is formed from the neighboring active vectors I_γ and I_δ, which have duty cycles of d_γ and d_δ, respectively. If the input currents are assumed to be constant over a switching period T_{sw}, the reference current vector is as follows.

$$I_{in} = d_\gamma I_\gamma + d_\delta I_\delta + d_0 I_0 \tag{4}$$

The calculation of the duty cycles d_γ and d_δ are relative to the currents I_γ and I_δ, are given by the following equations:

$$d_\gamma = \frac{t_{r1}}{T_{sw}} = m_R \sin\left(\frac{\pi}{3} - \theta_i\right) \tag{5}$$

$$d_\delta = \frac{t_{r2}}{T_{sw}} = m_R \sin\left(\theta_i\right) \tag{6}$$

$$d_0 = 1 - d_\gamma - d_\delta \tag{7}$$

Where, m_R is modulation factor; $0 \le m_R \le 1$

In the case where the null vector is eliminated from the switching sequence and the duty cycles are scaled back to the unit so as to satisfy the following expression:

$$I_{in} = d_\gamma^R I_\gamma + d_\delta^R I_\delta \tag{8}$$

The adjusted duty cycles of the rectifier stage are determined by the relationship (9), (10), where the modulation index $m_R = 1$ for maximum voltage at the DC bus [21]:

$$d_\gamma^{'} = \frac{d_\gamma}{d_\gamma + d_\delta} \tag{9}$$

$$d_\delta^{'} = \frac{d_\delta}{d_\gamma + d_\delta} \tag{10}$$

2.2.2 Inverter stage control

The three-phase output voltage inverter can, like any three-phase quantity (v_{Ak}, v_{Bk}, v_{Ck}) be decomposed into three other quantities: direct V_α, inverse V_β and homopolar V_0 using the Concordia or Park matrix [P(0)]. Since the voltage of each arm can only take two values, then there are eight possible combinations between these voltages for each inverter Figs. 4–6.

The principle of the space vector modulation control is to determine the output state of the inverter such that the three-phase system it generates, when brought back to two-phase, is approximately equal to the reference vector. Generally, the duty cycles d_α, d_β and d_0 for each inverter can be determined from Figs. 4–6.

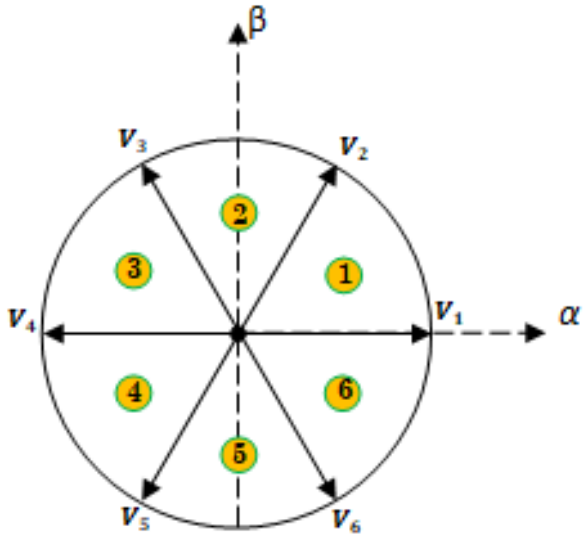

(a)

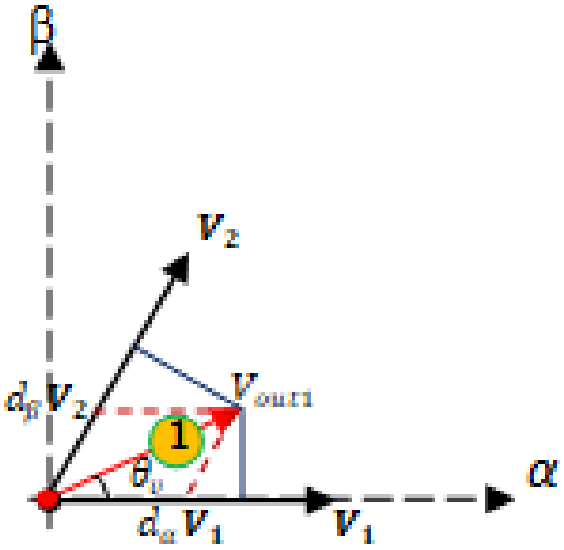

(b)

Fig. 4 Switching state vector of first voltage inverter (a) and its SVM in sector 1(b)

$$d_\alpha = \frac{T_\alpha}{T_{sw}} = m_v \cdot \sin\left(\frac{\pi}{3} - \theta_v\right) \tag{11}$$

$$d_\beta = \frac{T_\beta}{T_{sw}} = m_v \cdot \sin\left(\theta_v\right) \tag{12}$$

$$d_0 = 1 - d_\alpha - d_\beta \tag{13}$$

Where, m_v is modulation factor, $0 \le m_v \le 1$.

Finally, coordination between the control switches of the rectifier and the switches of the inverter is required to manage the indirect matrix converter under the restrictions

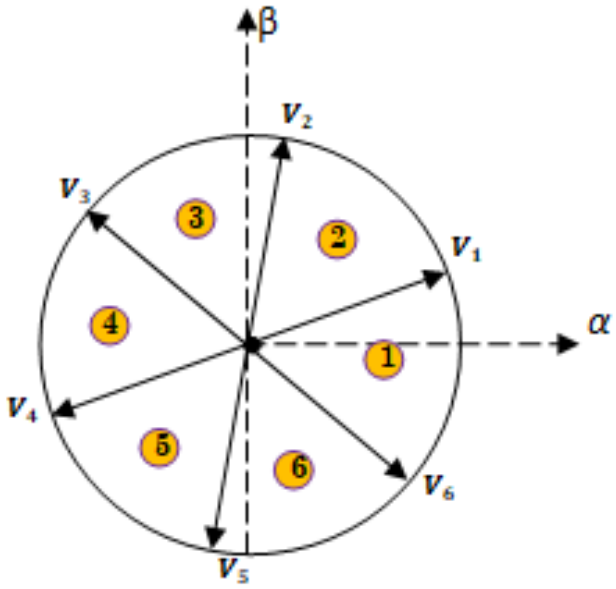

(a)

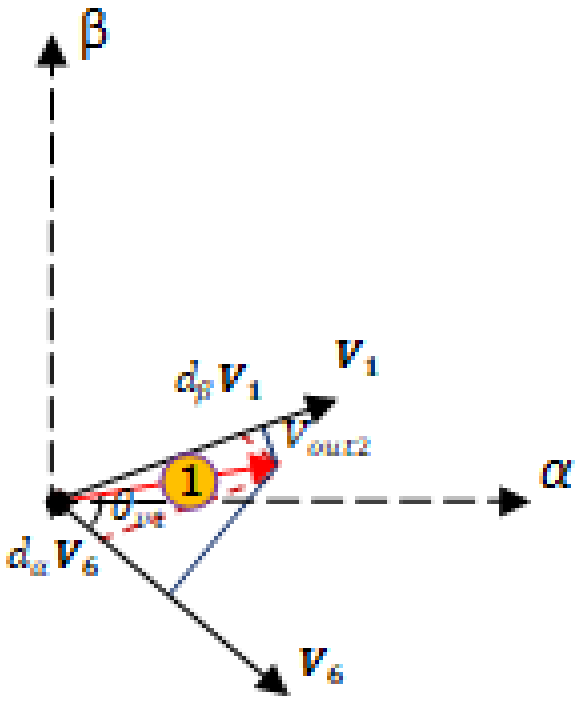

(b)

Fig. 5 Switching state vector of the second voltage inverter (a) and its SVM in sector 1(b)

of a variable input power factor, the two-way transit of power, and zero-current switching commutation. When the current is zero, the rectifier level is activated. Fig. 7 shows a control cycle during the sector **2** for the input current and sector **1** for the output voltage to demonstrate this coordination. The active vectors of the first inverter may

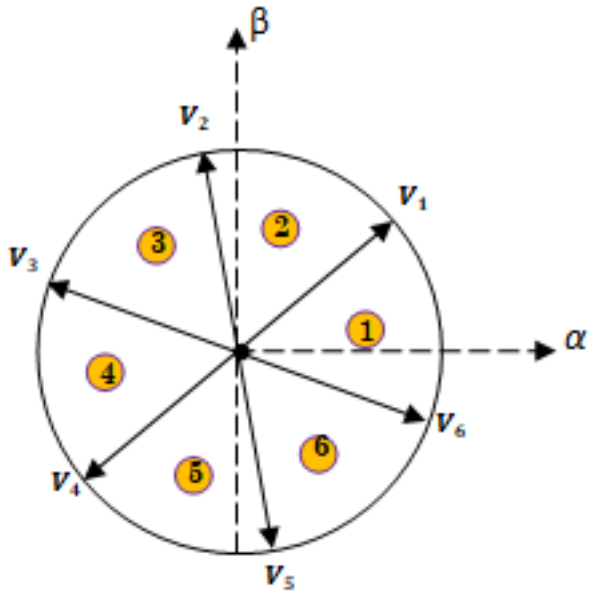

(a)

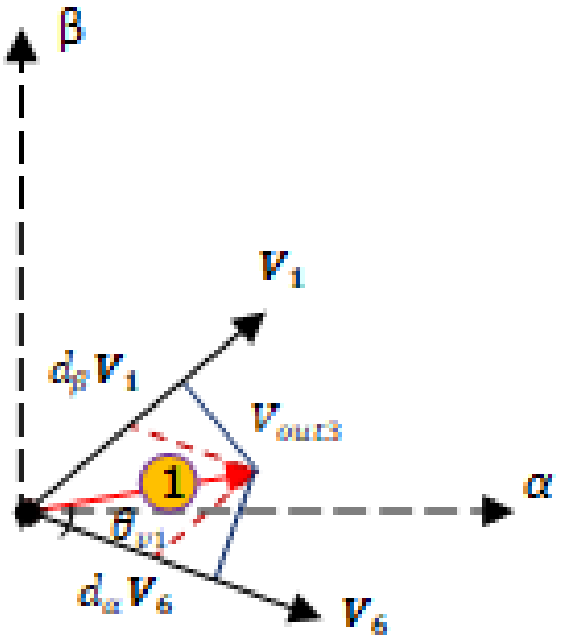

(b)

Fig. 6 Switching state vector of the third voltage inverter (a) and its SVM in sector **1** (b)

obviously be applied to the second one while taking into account the shifted angle of $\pi/9$ between them. Therefore, the following relationships can be used to obtain the duty ratios that correspond to the inverters stage [22]:

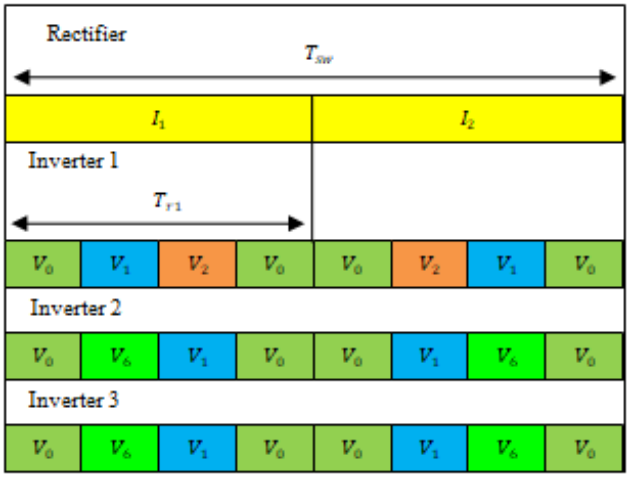

Fig. 7 Switching sequences of IMC (input current sector **2** and output voltage sector **1**)

$$\begin{cases} t_{r1} = d_{\gamma}^{R} \cdot T_{sw} \\ t_{i1} = \dfrac{1}{2} d_{\gamma}^{R} \cdot d_0 \cdot T_{sw} \\ t_{i2} = d_{\gamma}^{R} \cdot d_{\alpha} \cdot T_{sw} \\ t_{i3} = d_{\gamma}^{R} \cdot d_{\beta} \cdot T_{sw} \\ t_{i4} = \dfrac{1}{2} d_{\delta}^{R} \cdot d_0 \cdot T_{sw} \\ t_{i5} = \dfrac{1}{2} d_{\delta}^{R} \cdot d_{\beta} \cdot T_{sw} \\ t_{i6} = \dfrac{1}{2} d_{\delta}^{R} \cdot d_{\alpha} \cdot T_{sw} \end{cases} \tag{14}$$

3 Field-orientd control (FOC) for TSIM

The field-oriented control works in the same way that an independently excited DC motor does. Both the current and the torque can be adjusted individually in this motor. PI regulators are all that is needed to implement the control algorithm. If the induction motor's coordinate system is tied to the rotor's flux vector, flux and torque can indeed be controlled independently.

To summarize, Fig. 8 shows an illustration of the IFOC in a block form for TSIM. The main components of this type of control are the speed control loop, the θ_s calculation block and the direct PARK transformations. Speed is regulated through the block's external loop. The output of its regulator is the reference electromagnetic torque T_{em}^{*} or the reference currents i_{sq}^{*}. Parallel to this internal loop is a control loop for i_{sd}^{*}. The reference i_{sd}^{*} currents are calculated from the flux to be imposed. This

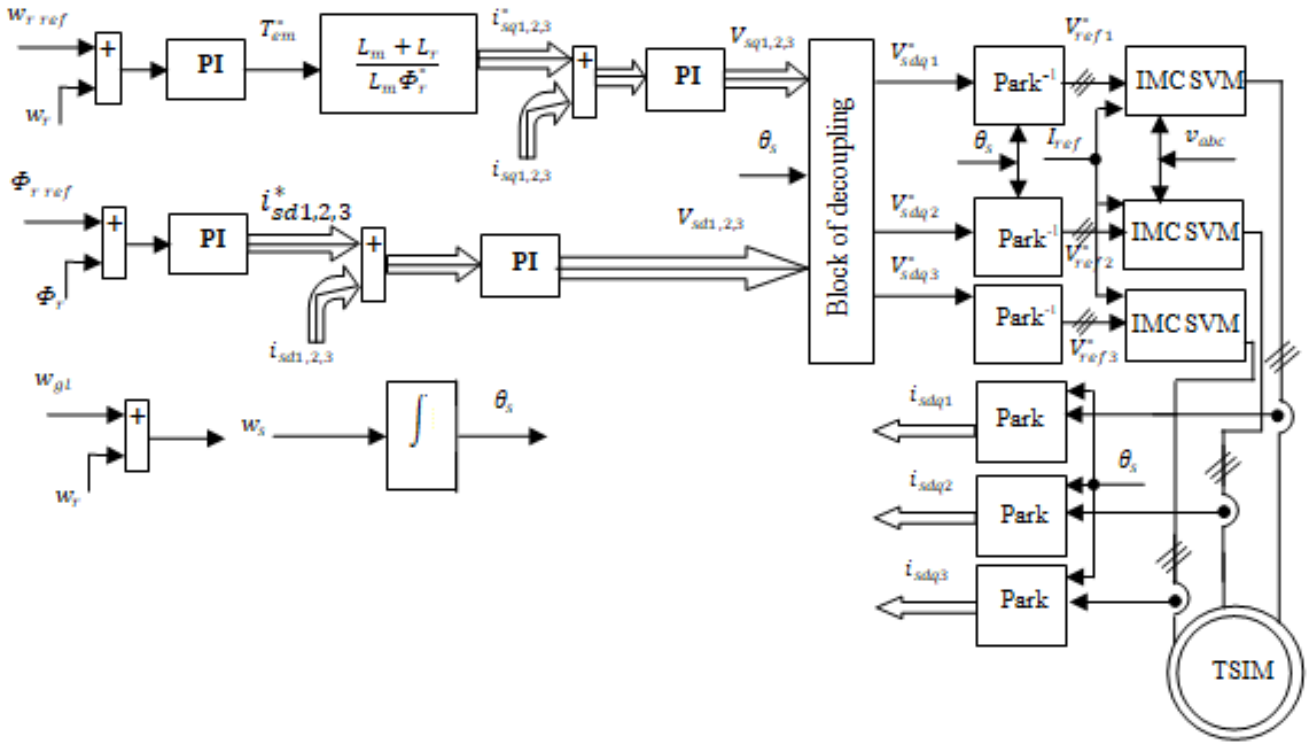

Fig. 8 An illustration of the IFOC in a block form for TSIM

flux corresponds to its nominal value for the speed range below the base speed and finally, the inverse PARK.

Fig. 9 depicts the *d-q* rotational coordinate system.

In our case, a *d-q* frame that rotates with the rotor flux vector Φ_r is chosen. This yields Eq. (15) shown below:

$$\begin{cases} \Phi_{rd} = \Phi_r \\ \Phi_{rq} = 0 \end{cases} \tag{15}$$

By imposing, $\Phi_{rd} = \Phi_r$ and $\Phi_{rq} = 0$, the TSIM equations in a reference frame related to the rotating field become:

$$\begin{cases} V_{sd1} = R_{s1} i_{sd1} + \dfrac{d\Phi_{sd1}}{dt} - w_s \Phi_{sq1} \\ V_{sq1} = R_{s1} i_{sq1} + \dfrac{d\Phi_{sq1}}{dt} - w_s \Phi_{sd1} \\ V_{sd2} = R_{s1} i_{sd2} + \dfrac{d\Phi_{sd2}}{dt} - w_s \Phi_{sq2} \\ V_{sq2} = R_{s1} i_{sq2} + \dfrac{d\Phi_{sq2}}{dt} - w_s \Phi_{sd2} \\ V_{sd3} = R_{s1} i_{sd3} + \dfrac{d\Phi_{sd3}}{dt} - w_s \Phi_{sq3} \\ V_{sq3} = R_{s1} i_{sq3} + \dfrac{d\Phi_{sq3}}{dt} - w_s \Phi_{sd3} \\ 0 = R_r i_{rd} + \dfrac{d\Phi_r}{dt} \\ 0 = R_r i_{rd} + (w_s - w_r)\Phi_r \end{cases} \tag{16}$$

with

$$\begin{cases} \Phi_{sd1} = L_{sd1} i_{sd1} + L_m (i_{sd1} + i_{sd2} + i_{sd3} + i_{rd}) \\ \Phi_{sq1} = L_{sq1} i_{sq1} + L_m (i_{sq1} + i_{sq2} + i_{sq3} + i_{rq}) \\ \Phi_{sd2} = L_{sd2} i_{sd2} + L_m (i_{sd1} + i_{sd2} + i_{sd3} + i_{rd}) \\ \Phi_{sq2} = L_{sq2} i_{sq2} + L_m (i_{sq1} + i_{sq2} + i_{sq3} + i_{rq}) \\ \Phi_{sd3} = L_{sd3} i_{sd3} + L_m (i_{sd1} + i_{sd2} + i_{sd3} + i_{rd}) \\ \Phi_{sq3} = L_{sq3} i_{sq3} + L_m (i_{sq1} + i_{sq2} + i_{sq3} + i_{rq}) \\ \Phi_r = L_r i_{rd} + L_m (i_{sd1} + i_{sd2} + i_{sd3} + i_{rd}) \\ 0 = L_r i_{rq} + L_m (i_{sq1} + i_{sq2} + i_{sq3} + i_{rq}) \end{cases} \tag{17}$$

The expression of the electromagnetic torque will in this case have the following form:

$$T_{em} = \frac{L_m}{L_r + L_m} P\left(\Phi_r \left(i_{sq1} + i_{sq2} + i_{sq3}\right)\right) \tag{18}$$

From the Eq. (7) of the two systems (16) and (17), the expression of the rotor flux becomes

$$\frac{d\Phi_r}{dt} = \frac{r_r L_m}{(L_m + L_r)}\left(i_{sd1} + i_{sd2} + i_{sd3}\right) - \frac{r_r}{(L_m + L_r)}\Phi_r \tag{19}$$

From Eqs. (18) and (19) one can see that if the rotor flux is kept constant, the torque depends solely on the quadrature component ($i_{sq1} + i_{sq2} + i_{sq3}$), while only the direct component ($i_{sd1} + i_{sd2} + i_{sd3}$) influences the amplitude of the rotor flux. As a result, a structure that is comparable to that of a separately excited MCC is produced.

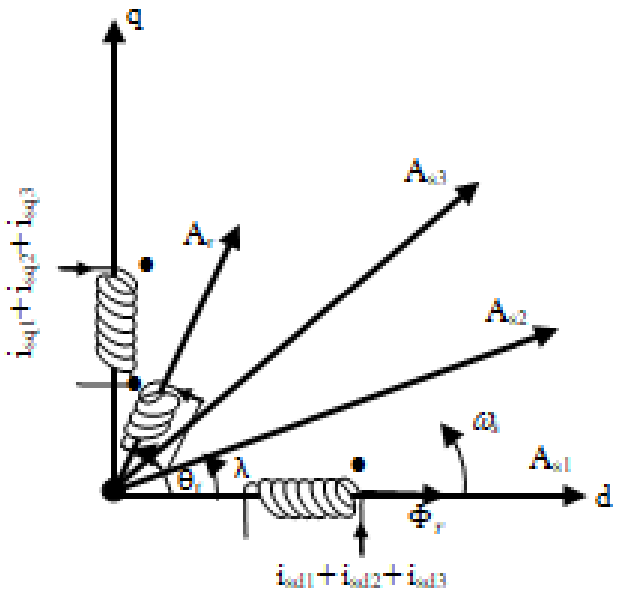

Fig. 9 Position of the frame to the rotor flux vector

The FOC is essentially based on the use of a coordinate transformation system. The latter requires the knowledge of the PARK angle θ_s. Depending on how this angle is determined. Two types of FOC techniques can be distinguished: the direct and indirect field oriented control (DFOC, IFOC) [6–9].

Unlike DFOC, IFOC does not use the magnitude of the rotor flux but only its position [8, 9]. It eliminates the need for a flux sensor or estimator or observer, but requires the use of a speed sensor. The phase of the flux is then determined using a mathematical model that can be incorporated into the control structure. The PARK angle θ_s is calculated from the stator pulsation, which is itself reconstructed using the machine speed and the rotor pulsation w_r.

$$w_s = w_{gl} + Pw_r \tag{20}$$

Where, w_{gl} denotes the slip angular speed. It is available as follows:

$$w_{gl} = \frac{1}{\left(i_{sd1}+i_{sd2}+i_{sd3}\right)} \frac{R_r}{\left(L_r+L_m\right)} \left(i_{sq1}+i_{sq2}+i_{sq3}\right) \tag{21}$$

4 Simulation results

To demonstrate the effectiveness of the proposed method, a numerical simulation of the dynamic behaviour of TSIM (Appendix Table A.1) fed by indirect matrix converters and controlled by IFOC is performed. The simulation parameters are: The reference flux $\Phi_{rref} = 1$ web, $T_L = 14$ N m for $2 \le$ t(s) ≤ 3; $w_{rref} = 157.07$ rps for $0 \le t(s) \le 3.5$ and $w_{rref} = -157.07$ rps for $3.5 \le t(s) \le 5$.

The electrical rotor speed is depicted in Fig. 10. It can be noticed that it tracks precisely its reference. The rotor speed keeps tracking its reference even in case of load torque variation (T_L = 14N m for $2 \le t(s) \le 3$) and speed reference modification from $w_{rref} = 157.07$ rps to $w_{rref} = -157.07$ rps at $t = 3.5$ s.

The rotor flux waveforms in *d-q* axis components are shown in Figs. 11 and 12, it is clear that the both Φ_d and Φ_q reach their references and remain almost constant which it guarantees the decoupling between the rotor speed, electromagnetic torque and the rotor flux.

Figs. 13–16 show simulation results for the torque dynamic, the stator currents *d-q* axis components i_{sq1}, i_{sq2}, and i_{sq3}, respectively, one can see that the Electromagnetic torque form is the same as the $i_{sq1,2,3}$ currents and follows the Electromagnetic torque reference.

Figs. 17 and 18 show the waveforms of the stator currents and their zoom.

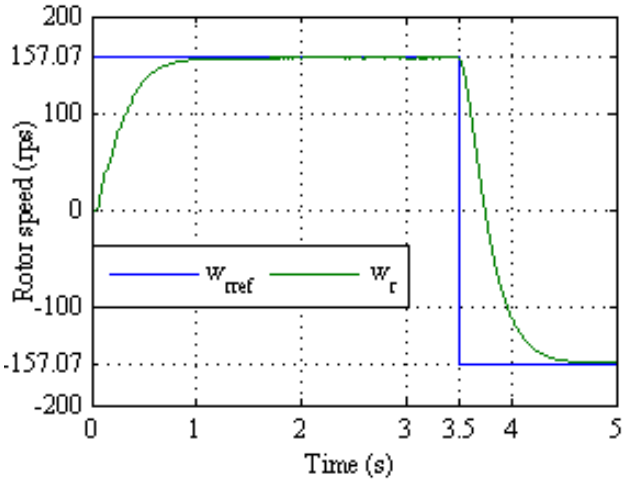

Fig. 10 Rotor speed

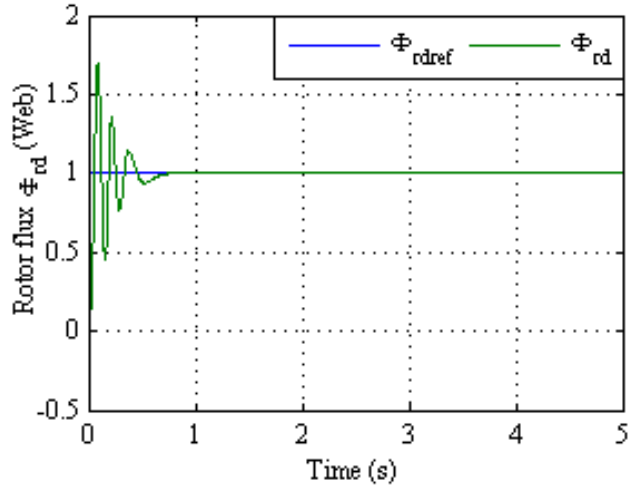

Fig. 11 Allure of direct rotor flux Φ_{rd}

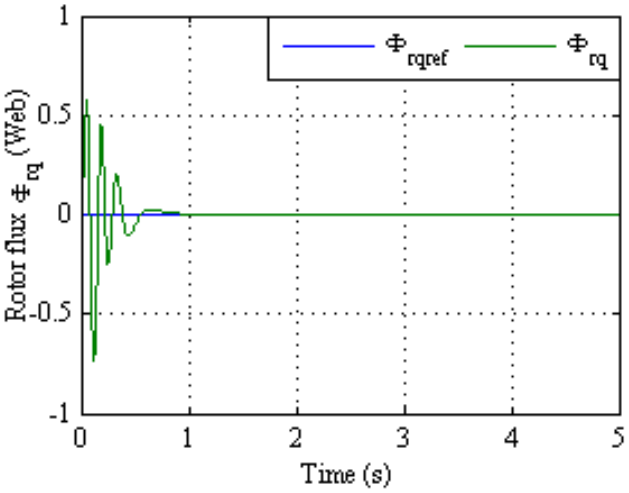

Fig. 12 Allure of quadrature rotor flux Φ_{rq}

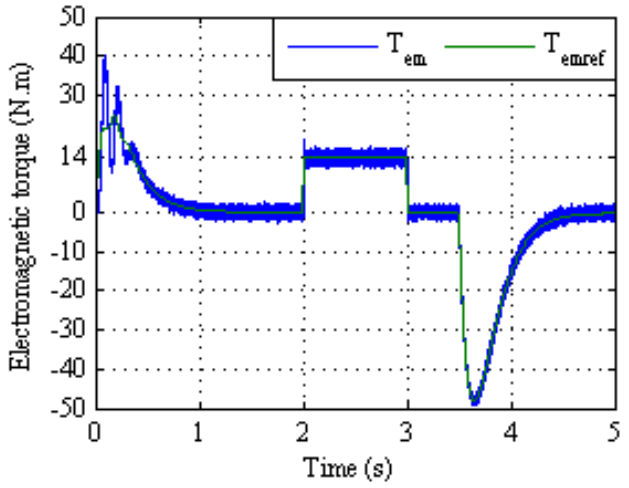

Fig. 13 Electromagnetic torque trajectory

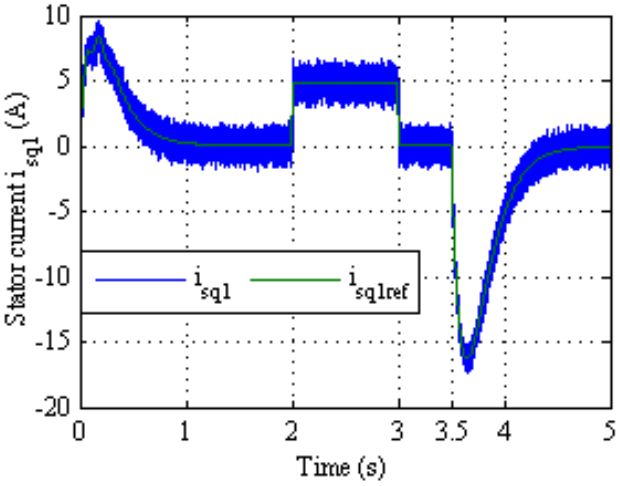

Fig. 14 Stator current i_{sq1} waveform

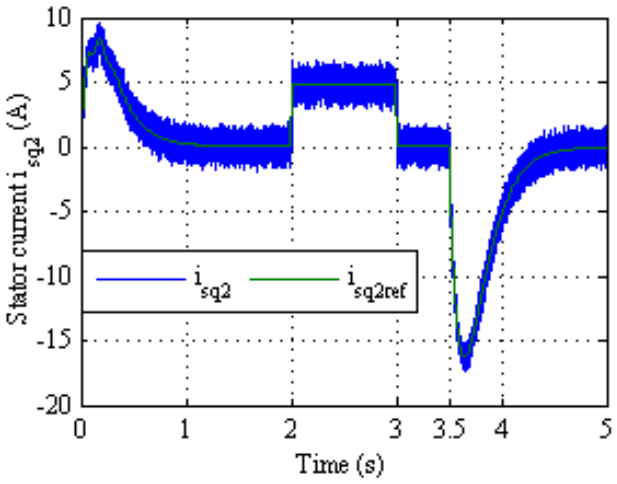

Fig. 15 Stator current i_{sq2} waveform

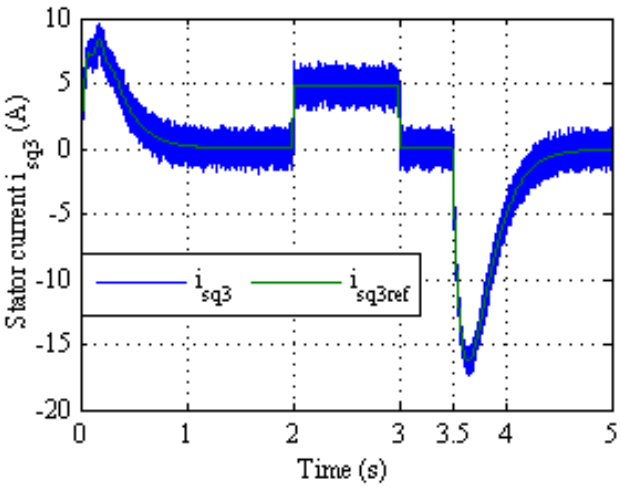

Fig. 16 Stator current i_{sq3} waveform

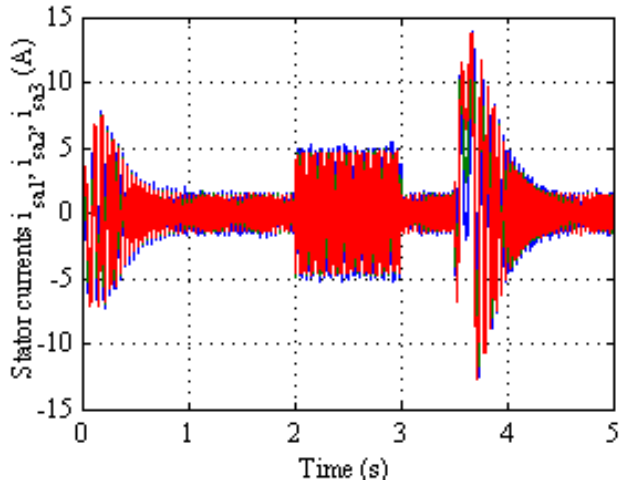

Fig. 17 Stator currents waveforms

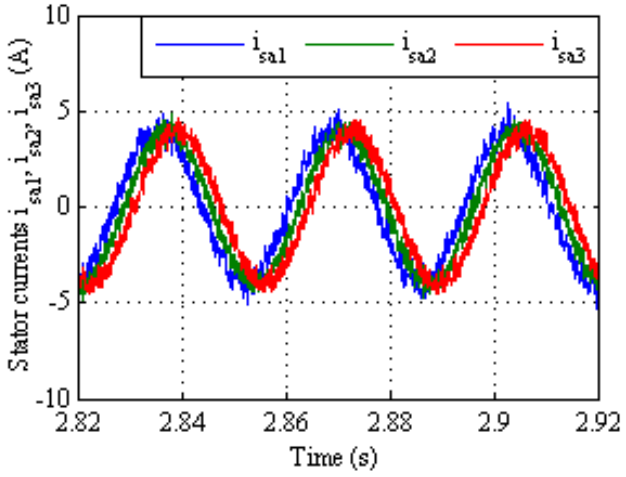

Fig. 18 Zoom of stator currents waveforms

Figs. 19 and 20 illustrate the DC link voltage waveform and the indirect matrix output voltage waveform.

Finally, Figs. 21 and 22 depict the input voltage, current, and filtered input current, respectively. As it can be seen, the control has a unity input power factor.

5 Conclusions

The efficiency of an indirect field oriented control controlled triple star induction motor (TSIM) with an indirect matrix converter is investigated in this paper. The converter is composed of three inverters linked by a fictitious DC link to a standard bidirectional current source rectifier. For the converter, a space vector modulation was envisaged; in this method, three conventional SVM of indirect matrix converters with particular switching vector location patterns are used. In the rectifier stage, the space vector modulation strategy results in an adjustable input displacement power factor and near sinusoidal input current. The simulation findings showed the decoupling of motor speed and rotor flux while maintaining excellent drive performance and a power factor at unity. Add to this the benefits of the IFOC, which ensures precise decoupling between rotor flux and motor speed in dynamic and steady states.

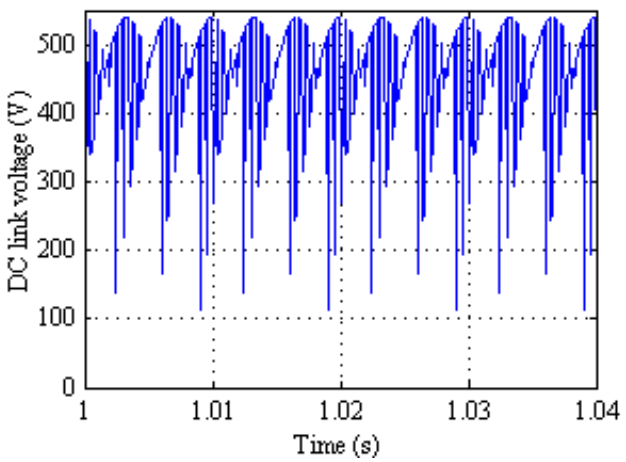

Fig. 19 DC link voltage

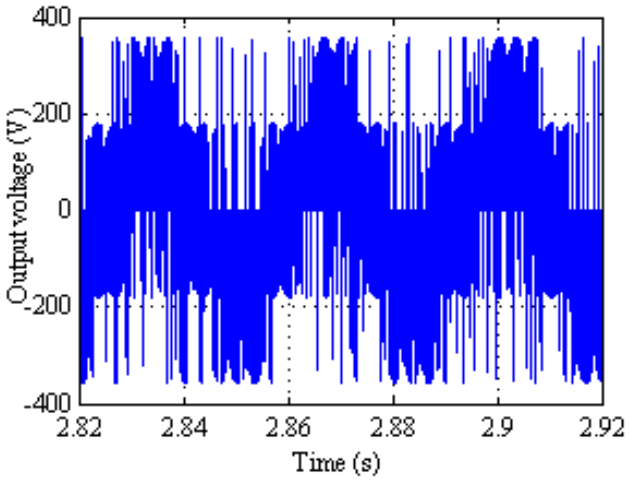

Fig. 20 Output IMC voltage waveform

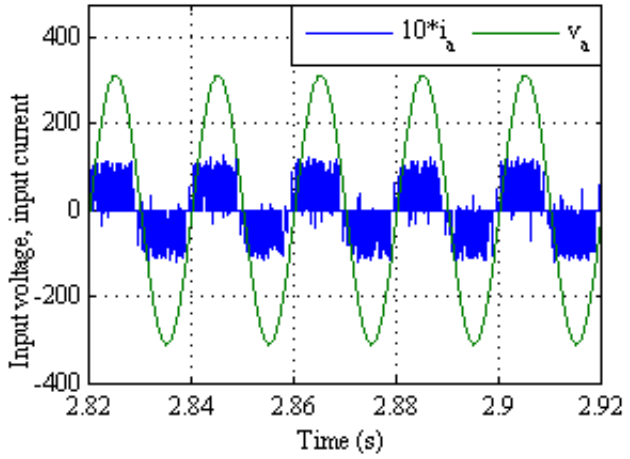

Fig. 21 Input voltage and input current

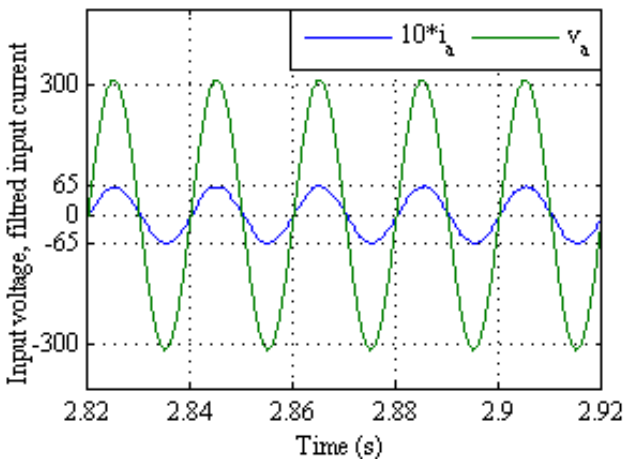

Fig. 22 Input voltage and filtered input current

References

[1] Levi, E., Bojoi, R., Profumo F., Toliyat, H. A., Williamson, S. "Multiphase induction motor drives - A technology status review", IET Electric Power Applications, 1(4), pp. 489–516, 2007. https://doi.org/10.1049/iet-epa:20060342

[2] Levi, E. "Multiphase electric machines for variable-speed applications", IEEE Transations on Industrial Electronics, 55(5), pp. 1893–1909, 2008. https://doi.org/10.1109/TIE.2008.918488

[3] Rubino, S., Mandrile, F., Armando, E., Bojoi, I. R., Zarri, L. "Fault-Tolerant Torque Controller Based on Adaptive Decoupled Multi-Stator Modeling for Multi-Three-Phase Induction Motor Drives", IEEE Transactions on Industry Applications, 58(6), pp. 7318–7335, 2022. https://doi.org/10.1109/TIA.2022.3197547

[4] Rubino, S., Bojoi, R., Cittanti, D., Zarri, L. "Decoupled and Modular Torque Control of Multi-Three-Phase Induction Motor Drives", IEEE Transactions on Industry Applications, 56(4), pp. 3831–3845, 2020. https://doi.org/10.1109/TIA.2020.2991122

[5] Rubino, S., Bojoi, R., Cittanti, D., Zarri, L. "Decoupled torque control of multiple three-phase induction motor drives", In: IEEE Energy Conversion Congress and Exposition (ECCE), Baltimore, MD, USA, 2019, pp. 4903–4910. ISBN 9781728103969 https://doi.org/10.1109/ECCE.2019.8912502

[6] Blaschke, F. "The Principle of Field Orientation as Applied to the NEW Transvector Closed-Loop System for Rotating-Field Machines", Siemens Review, 34, pp. 217–220, 1972.

[7] Amimeur, H., Abdessemed, R., Aouzellag, D., Merabet, E., Hamoudi, F. "A Sliding Mode Control associated to the Field-Oriented Control of Dual-Stator Induction Motor Drives", Journal of Electrical Engineering, 10(3), pp. 7–12, 2010. [online] Available at: http://www.jee.upt.ro/index.php/jee/article/view/WM1260085278W4b1b601edb399/357 [Accessed: 02 April 2023]

[8] Andriamalala, R. N., Razik, H., Sargos, F. M. "Indirect-Rotor-Field-Oriented-Control of a Double-Star Induction Machine using the RST controller", In: 2008 34th Annual Conference of IEEE Industrial Electronics, Orland, FL, USA, 2008, pp. 3108–3113. https://doi.org/10.1109/IECON.2008.4758457

[9] Lekhchine, S., Bahi, T., Soufi, Y. "Indirect rotor field oriented control based on fuzzy logic controlled double star induction machine", International Journal of Electrical Power & Energy Systems, 57, pp. 206–211, 2014. https://doi.org/10.1016/j.ijepes.2013.11.053

[10] Amimeur, H., Aouzellag, D., Abdessemed, R., Ghedamsi, K. "Sliding mode control of a dual-stator induction generator for wind energy conversion systems", International Journal of Electrical Power & Energy Systems, 42, pp. 60–70, 2012. https://doi.org/10.1016/j.ijepes.2012.03.024

[11] Yoon, Y.-D., Sul, S.-K. "Carrier-Based Modulation Technique for Matrix Converter", IEEE Transactions on Power Electronics, 21(6), pp. 1691–1703, 2006. https://doi.org/10.1109/TPEL.2006.882935

[12] Cardenas, R., Peña, R., Wheeler, P., Clare, J. "Experimental Validation of a Space-Vector-Modulation Algorithm for Four-Leg Matrix Converters", IEEE Transactions on Power Electronics, 58(4), pp. 1282–1293, 2011. https://doi.org/10.1109/TIE.2010.2068531

[13] Wheeler, P. W., Rodriguez, J., Clare, J. C., Empringham, L., Weinstein, A. "Matrix converter: a technology review", IEEE Transactions on Power Electronics, 49(2), pp. 276–288, 2002. https://doi.org/10.1109/41.993260

[14] Wang, B., Venkataramanan, G. "A carrier-based PWM algorithm for indirect matrix converters", In: 37th IEEE Power Electronics Specialists Conference, Jeju, South Korea, 2006, pp. 1–8. ISBN 0-7803-9716-9 https://doi.org/10.1109/pesc.2006.1712191

[15] Itoh, J. I., Hinata, T., Kato, K., Ichimura, D. "A novel control method to reduce an inverter stage loss in an indirect matrix converter", In: 2009 35th Annual Conference of IEEE Industrial Electronics, pp. 4475–4480. ISBN 9781424446490 https://doi.org/10.1109/IECON.2009.5414884

[16] Kolar, J. W., Baumann, M., Schafmeister, F., Ertl, H. "Novel three-phase AC–DC–AC sparse matrix converter", In: APEC. Seventeenth Annual IEEE Applied Power Electronics Conference and Exposition (Cat. No.02CH37335), Dallas, TX, USA, 2002, pp. 777–791. ISBN 0-7803-7404-5

[17] Kolar, J. W., Schafmeister, F., Round, S. D., Ertl, H. "Novel three-phase AC–AC sparse matrix converters", IEEE Transactions on Power Electronics, 22(5), pp. 1649–1661, 2007. https://doi.org/10.1109/TPEL.2007.904178

[18] Patel, P. P., Mulla, M. A. "A Single Carrier-Based Pulsewidth Modulation Technique for Three-to-Three Phase Indirect Matrix Converter", IEEE Transactions on Power Electronics, 35(11), pp. 11589–11601, 2020. https://doi.org/10.1109/TPEL.2020.2988594

[19] Varajão, D., Araújo, R. E. "Modulation methods for direct and indirect matrix converters: A review", Electronics, 10(7), 812, 2021. https://doi.org/10.3390/electronics10070812

[20] Nguyen, T. D., Lee, H. H. "Dual Three-Phase Indirect Matrix Converter With Carrier-Based PWM Method", IEEE Transactions on Power Electronics, 29(2), pp. 569–581, 2013. https://doi.org/10.1109/TPEL.2013.2255067

[21] Nguyen, T. D., Lee, H. H. "Modulation Strategies to Reduce Common-Mode Voltage for Indirect Matrix Converters", IEEE Transactions on Industrial Electronics, 59(1), pp. 129–140, 2011. https://doi.org/10.1109/TIE.2011.2141101

[22] Lavanya, N., Venu Gopala Rao, M. "Control of Indirect Matrix Converter With Improved SVM Method", International Journal Of Power Electronics And Drive Systems, 6(2), pp. 370–375, 2015. https://doi.org/10.11591/ijpeds.v6.i2.pp370-375

Appendix

Table A.1 Parameters of 4.5 Kw three-star induction motor

Power	P_n = 4.5 Kw
Based speed	N_r = 2922 rpm
Stator winding resistance	R_s = 3.75 Ω
Stator winding resistance	R_r = 2.12 Ω
Stator leakage inductance	L_{ls} = 0.022 H
Rotor leakage inductance	L_{lr} = 0.006 H
Mutual inductance	L_m = 0.3672 H
Number of pole pairs	P = 1
Moment of inertia	J = 0.0625 Kg m^2

Table A.2 Nomenclature, Greek letters and abbreviations

Nomenclature	
A_{s1}, B_{s1}, C_{s1} A_{s2}, B_{s2}, C_{s2}, A_{s3}, B_{s3}, C_{s3}	Three TSIM stator winding systems.
A_r, B_r, C_r	Rotor winding system
v_j (j = a, b, c)	Single voltages relative to grid neutral
v_p, v_n	Positive and negative potential of the fictitious IMC DC bus
v_j (j = Ak, Bk, Ck)	Single voltages with respect to TSIM neutral
t_1, t_2, t_3, t_0	The application times of the vectors bordering a sector and the zero vector
T_{sw}	Switching period
V_{sd1}, V_{sq1}, V_{sd2}, V_{sq2}, V_{sd3}, V_{sq3}	Star voltages 1, 2 and 3 in PARK reference frame (d, q)
V_{rd}, V_{rq}	Rotor voltages in PARK reference frame (d, q)
i_{sd1}, i_{sq1}, i_{sd2}, i_{sq2}, i_{sd3}, i_{sq3}	Star currents 1, 2 and 3 in PARK reference frame (d, q)
i_{rd}, i_{rq}	Rotor currents in PARK reference frame (d, q)
i^*_{ds1}, i^*_{qs1}, i^*_{ds2}, i^*_{qs2}, i^*_{ds3}, i^*_{qs4}	Reference currents of star 1, 2 and 3 in PARK reference frame
w_r, w_{rref}	Fundamental electrical pulse of rotor magnitudes and its reference
T_{em}, T^*_{em}	Electromagnetic torque and its reference
Greek letters	
α, β	Stator reference frame
d_γ, d_δ	Input current vector duty cycle I_γ, I_δ
d^R_γ, d^R_δ	Adjusted input current vector duty cycle I_γ, I_δ
d_α, d_β	Output voltage vector duty cycle V_α, V_β
Φ_{sd1}, Φ_{sq1}, Φ_{sd2}, Φ_{sq2}, Φ_{sd3}, Φ_{sq3},	Star flux 1, 2 and 3 in PARK's reference frame (d, q)
Φ_{rd}, Φ_{rq}	Rotor flux in the PARK frame of reference (d, q)
θ_s	PARK angle
Φ_r, Φ_{rref}	TSIM rotor flux vector and its reference
Abbreviations	
IMC	Indirect matrix converter
VSI	Voltage source inverter
CM	Matrix converter
FOC	Field oriented control
TSIM	Triple star induction motor
SVM	Space vector modulation